Molecular Genetics & Genomic Medicine

WILEY

Molecular Genetics & Genomic Medicine
Open Access

ORIGINAL ARTICLE OPEN ACCESS

A Novel Mutation Located in the N-Terminal Domain of MYO15A Caused Sensorineural Hearing Loss

Yanli Wang[1] | Zengping Liu[1] | Yong Li[1] | Zhipeng Nie[2] | Baicheng Xu[1] | Yiming Zhu[1] | Shihong Duan[1] | Xingjian Chen[1] | Huan Tan[1] | Jiong Dang[1] | Minxin Guan[2] | Yufen Guo[1]

[1]Department of Otolaryngology—Head and Neck Surgery, Lanzhou University Second Hospital, Lanzhou, Gansu, China | [2]Institute of Genetics, Zhejiang University School of Medicine, Zhejiang, Hangzhou, China

Correspondence: Minxin Guan (gminxin88@zju.edu.cn) | Yufen Guo (guoyflz@163.com)

Received: 30 July 2024 | **Revised:** 7 November 2024 | **Accepted:** 12 November 2024

Funding: This work was supported by grants from the National Natural Science Foundation of China (Yufen Guo, Grant 82160214 and Yanli Wang, Grant 82360221), the Doctoral Tutor Project of Lanzhou University Second Hospital (Yufen Guo, Grant bdkyjj-02), and the Natural Science Foundation of Gansu Province (Yanli Wang, Grant 22JR11RA065).

Keywords: deafness | hair cell-like cell | induced pluripotent stem cells (iPSCs) | *MYO15A* | novel mutation

ABSTRACT

Background: *MYO15A* is one of the common genes of severe-to-profound sensorineural deafness. Mutations in this gene can cause both pre- and post-lingual hearing losses. In this study, a novel *MYO15A* variant (c.2482C>T) was identified to be associated with autosomal recessive non-syndromic hearing loss (ARNSHL) in a Chinese Uighur family.

Methods: To examine the effects of the *MYO15A* mutation on the morphology and function of the derived hair cell-like cells, two iPSCs were generated separately from the proband and a mutation-negative family member and those were then induced to hair cell-like cells.

Results: Results showed that this homozygous *MYO15A* mutation (PVS1 + PM2 + PP1 + PP3), which is located in the N-terminal domain, displayed significant differences in the morphology and function of hair cell-like cells between the proband and the normal control, although it had no effect on the totipotency of iPSCs.

Conclusion: Our study demonstrates that the novel variant c.2482C>T in the *MYO15A* gene may cause inner ear hair cell dysfunction and audiological disorders in this family.

1 | Introduction

Hearing loss is a common disorder that causes difficulty in communication; more than 50% of congenital deafness cases are caused by genetic factors, with autosomal recessive deafness being the most common (Bitner-Glindzicz 2002). Over 77 genes display relationships to autosomal recessive non-syndromic hearing loss (ARNSHL) (https://hereditaryhearingloss.org/, updated in 08/30/2021). Among these genes, the *MYO15A* gene is considered to be the third- or fourth-most frequent cause of ARNSHL (Rehman et al. 2016). In 1998, *MYO15A* mutations were first identified in three ARNSHL families in Indonesia and India (Wang et al. 1998); since then, a fast-growing number of *MYO15A* variants relating to auditory phenotypes, including milder, severe, or profound hearing loss, have been reported around the world; to date, over 240 *MYO15A* variants associated with DFNB3 have been described (Zhang et al. 2019). The frequency of *MYO15A* mutations varied in different regions across the world, with approximate 4.9% among patients with ARNSHL (Farjami et al. 2020).

Yanli Wang and Zengping Liu contributed equally to this work and share first authorship.

Inner ear hair cells are the main auditory receptors (Hudspeth 2014; Chen et al. 2016), in which the proteins enriched play specific roles in the development and maintenance of the mechanical transduction devices (Scheffer et al. 2015). Myosin XVa (MYO15A, OMIM: 602666) that is encoded by *MYO15A* is essential for the maintenance of normal hearing and plays an indispensable role in the development of stereocilia and actin organization in hair cells of the inner ear (Redowicz 1999); mutations in *MYO15A* were recognized as one of the common causes leading to severe to profound ARNSHL (Rehman et al. 2016). In 2006, Takahashi and Yamanaka successfully induced pluripotent stem cells (iPSC) from mouse embryonic or adult fibroblasts by introducing four factors, Oct3/4, Sox2, c-Myc, and Klf4 (Takahashi and Yamanaka 2006). Two years later, the human-induced pluripotent stem cells were generated from dermal fibroblasts by the same method (Lowry et al. 2008). IPSC technology makes it easy and effective to harvest stem cells, which can then be used for further research or therapy; therefore, it has been widely used in the field of regenerative medicine.

In this manuscript, we identified a novel homozygous *MYO15A* mutation (c.2482C>T) located in the N-terminal domain associated with ARNSHL in a Chinese Uighur family. We also generated iPSCs from the proband and a family member without *MYO15A* mutation and then induced those iPSCs to hair cell-like cells. We found that only the homozygous *MYO15A* mutation from the proband resulted in abnormal morphology and dysfunction of the derived hair cell-like cells. Our data demonstrate that the novel mutation may cause inner ear hair cell dysfunction and audiological disorders in this family.

2 | Materials and Methods

2.1 | Ethical Compliance

Approvals in this study, including blood and skin samples, were approved by the ethics committee of Lanzhou University Second Hospital (no. 2023A-233).

2.2 | Participants and Clinical Characteristics

The blood samples came from 10 members of a Chinese family carrying the *MYO15A* mutation, and 861 genetically unrelated Chinese deaf patients were collected in this survey. In addition, a total of 200 blood samples from unaffected Chinese subjects from the same region were also recruited as a control group. Systematic clinical examination and audiometric assessments were performed on all participants in order to exclude any syndromic findings and genetic factors associated with hearing impairment in these subjects. The audiological examinations included pure-tone audiometry (PTA) and/or auditory brainstem response (ABR), immittance testing, and distortion product otoacoustic emission (DPOAE). The degree of hearing impairment was classified according to the air-conduction average hearing thresholds of the better ear at 500, 1000, 2000, and 4000 Hz. The severity of hearing impairment was classified into five grades: normal $\leq$25 dB HL; mild = 26–40 dB HL; moderate = 41–60 dB HL; severe = 61–80 dB HL; and profound $\geq$81 dB HL (http://www.who.int/pbd/deafness/hearing_impairment_grades/en/). Temporal bone high-resolution computed tomography (HRCT) was performed for the proband. Axial and coronal temporal bone CTs were carried out abiding by the recognized standards to define cochlea vestibular malformations (Sennaroglu and Bajin 2017).

2.3 | Identification of Pathogenic Variant

Identification of pathogenic variant was performed after genomic DNAs were extracted from acquired peripheral blood samples. Firstly, the proband II-2 was screened for hotspot variants in genes *GJB2*, *SLC26A4*, *GJB3*, and mitochondrial 12S rRNA, and no variants were found. Subsequently, whole exome sequencing (WES) was conducted in two affected members (II-2 and II-5) by Igenetech Biotech Co. Ltd. (Beijing) as detailed elsewhere (Cui et al. 2020). Finally, we filtered out the SNPs based on the criteria for potential candidate variants, including mutant allele frequency less than 1% in public databases, non-synonymous or in splice sites within 6 bps of a coding exon, and cosegregation with the phenotype. The pathogenicity of the suspected mutation was analyzed according to the ACMG guidelines.

The software Primer 5.0 was used to design primers for the flanking sequences of intron or exon where c.2482C>T is located. PCR was used to amplify targeting DNA fragments; each PCR fragment was purified and then directly sequenced, and the sequence data were compared with the NCBI *MYO15A* reference sequences (NM_016239.4) by Sequencher 5.4.5 software. The primers, all genotyping and sequencing, were performed at Tsingke Biotechnology Co. Ltd. (Beijing, China). DNA fragments of 10 family members, 861 genetically unrelated probands, and 200 control subjects were validated by Sanger sequencing.

2.4 | Induced Fibroblasts to iPSCs

Human epidermic tissues were obtained from donors' arms (II-2 and II-7) with a 6-mm skin punch (Vetlab Supply, Palmetto Bay, FL, USA). Primary fibroblasts were isolated and cultured according to the methods reported in the previous literatures (Chen et al. 2016; Park et al. 2008). The five episomal vectors, namely, pCXLEhOCT3/ 4-shp53-F (#27077), pCXLE-hSK(#27078), pCXLE-hUL(#27080), pCXLE-EGFP (#27082), and pCXWB-EBNA1(#37624) (0.5 μg per vector, Addgene, USA), were electroporated into fibroblasts (5×10^5 cells) to generate iPSCs (Okita et al. 2011). The electroporation was performed on the Lonza Nucleofector 2b device using program U-23 with Basic Nucleofector Kit for Primary Mammalian Epithelial Cells (Lonza). After electroporation, the cells were seeded in a 10-cm plate and cultured in high glucose DMEM (HyClone) medium supplemented with 10% FBS (Gibco), 1% of GlutaMax (Gibco), 1% of nonessential amino acids (Gibco), 1% of penicillin–streptomycin solution (Beyotime), 50 μg/mL of VitC (Sigma), and 100 μm/mL of BME (Sigma). From Day 2 to 6, the medium was replaced daily and the 5 μM/mL sodium butyrate (Sigma) was added. On Day 7, the cells were re-digested and transferred to 6-well plates precoated with Matrigel (Corning) at a density of 5×10^4 cells per well and cultured in mTeSR (Stem Cell Technologies) medium. From Day 7 to 12, 5 μM/mL of sodium butyrate was added to the medium

and the medium was replaced daily. After Day 12 and thereafter, the medium without sodium butyrate was changed every 2 days. The iPSC colonies can be observed in about 15 days later; then, these iPSC colonies were manually picked and cultured in mTeSR after 20–22 days. The iPSCs were routinely passaged with Accutase (Gibco) every 6 days at a 1:6 split ratio and placed in a 5% CO_2 incubator (Thermo Fisher Scientific) maintained at 37°C (Wen et al. 2021).

2.5 | Induction of iPSCs Toward Inner Ear Hair Cells

IPSCs were induced to differentiate into inner ear hair cells using a monolayer induction method (Chen et al. 2012). After 10–12 days of differentiation, otic epithelial progenitors (OEPs) can be observed and then collected for induced differentiation into hair cells for 3 weeks. When OEPs were induced toward hair cells, the cells were digested and collected and then seeded at a density of 1000 cell/cm^2 onto a culture dish precoated with Matrigel and pre-seeded with mitotically inactivated embryonic CUSCs on Day 18 (Oshima et al. 2010).

2.6 | Identification of iPSC Pluripotency

Cells grown on Matrigel-coated glass coverslips were fixed, permeabilized, incubated, stained with primary antibodies and secondary antibodies (IgG, Invitrogen), redyed with DAPI solution, and sealed with Dako fluorescence binder as the protocol previously reported (Cui et al. 2020).

For analysis of in vivo differentiation totipotency and tridermogenesis of the putative iPSCs, the iPSCs with Matrigel were, respectively, co-injected into the subcutaneous back and thigh muscles of NOD-SCID immunodeficient mice about 8 weeks old. About 8 weeks later, the mice were killed, and the teratoma was removed, fixed with 10% formaldehyde solution, and then HE (hematoxylin and eosin) staining was performed.

2.7 | Mycoplasma Testing

The mycoplasma PCR kit (Biyuntian, China) was used to test whether the iPSC cell lines were contaminated by mycoplasma by nested PCR.

2.8 | STR (Short Tandem Repeat) Testing

Fibroblasts and induced iPSC cell precipitates were sent to GENEWIZ Inc. (Suzhou, China) for matching testing at 10 sites.

2.9 | Gene Expression Analysis

The mRNA levels of the affected and unaffected cell lines were compared by RT-qPCR. The TRIzol reagent (Invitrogen, 15596026) was used to extract total cellular RNAs from various cells and tissues, and then PrimeScript II 1st Strand cDNA Synthesis Kit (Takara, 6210A) was used to reverse transcript into cDNA. The primers were designed on exon 2 based on isoform 1 (F: TCCCTACGACTACTACCACCC, R: TAAGGAGACGAGTACCCCGAC). The relative standard curve method was used to analyze target gene with Maxima SYBR Green/ROX qPCR Master Mix Kit (Fermentas). Expression was normalized to *GAPDH* in the same sample and was measured by three independent experiments. Reactions were carried out on Applied Biosystems 7900HT Fast Real-Time PCR System. The 7900 System SDS RQ Manager Software was used to analyze acquired data, *GAPDH* was used as a housekeeping gene, and the relative gene expression was measured by the $2^{-\Delta\Delta Ct}$ method.

2.10 | Scanning Electronic Microscopy (SEM)

The cells were fixed in 2.5% glutaraldehyde (Sigma-Aldrich) in PBS at 4°C overnight. PBS was used to wash three times for 15 min each time; then, cells were fixed in PBS with 1% OsO_4 for 2 h and subsequently washed three times for 15 min. Cells were then dehydrated with a graded ethanol series for 15 min each time. Samples were dehydrated twice in 100% ethanol before being transferred into isoamyl acetate for 1 h and dehydrated with liquid CO_2 in a Hitachi Model HCP-2 critical point dryer. Gold–palladium was coated with a Hitachi Model E-1010 ion sputter for 5 min. Finally, the samples were observed by a Hitachi SU8010 SEM (Chen et al. 2016). Multiple areas of hair cell-like cells (per 1 μm^2) were counted using ImageJ software ($n = 5$).

2.11 | Statistics

Statistical analysis was calculated using SPSS 19.0 software (SPSS Inc. Chicago, IL, USA). Assuming that $\alpha = 0.05$, if the $p < 0.05$, the difference was considered to be significant.

3 | Results

3.1 | Clinical Characterizations and Identification of MYO15A Mutation

We identified the pathogenic gene of a Chinese Uighur deafness family (JX81), which contained four of eight members with a bilateral profound non-syndromic sensorineural hearing loss (NSHL) (Figure 1). There was no any family history of systemic diseases. Detailed physical and clinical examinations including ABR, DPOAE, and temporal bone HRCT were performed on the proband, but no abnormalities were found. There was no inner ear malformations, acoustic neuroma, auditory neuropathy spectrum disorders, or incorporate other systemic abnormalities; all affected individuals presented with congenital preverbal deafness.

No mutations were identified in the initial screening of *GJB2*, *SLC26A4*, *GJB3*, and mitochondrial 12S rRNA. Genomic DNAs from two hearing-impaired family members (II-2 and II-5) were then selected to WES. After removing annotated polymorphisms and filtering for variants, only a single exonic variant (c.2482C>T, p.Arg828*) was identified in the exon 2

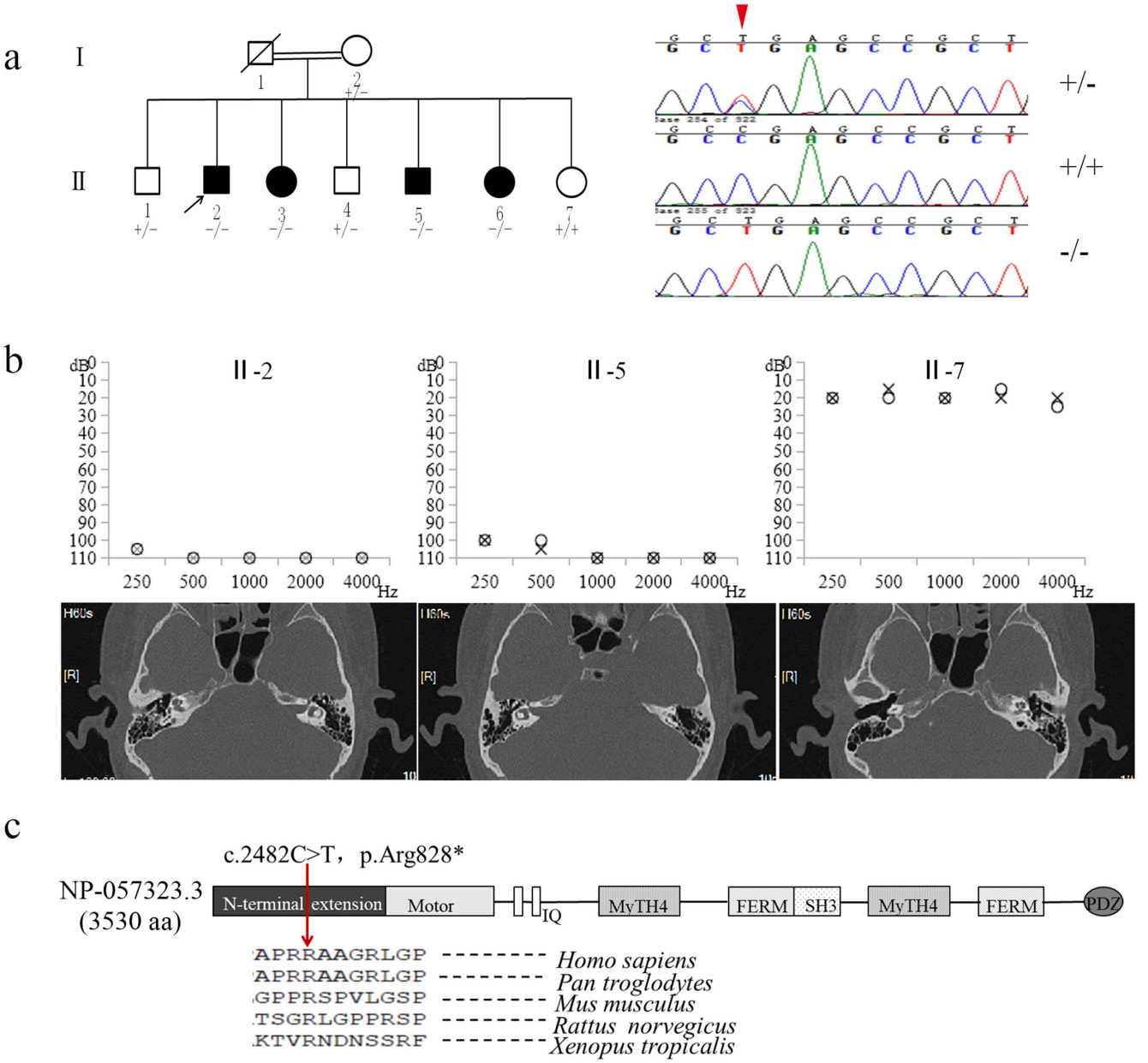

FIGURE 1 | Identification of *MYO15A* mutation. (a) Pedigree map and genotypes in a Chinese Uighur family carrying *MYO15A* mutation (c.2482C>T). Blackened symbols mean hearing-impaired individuals; the proband is identified by an arrow. The C/T transversion at the 2482 codon in Sanger sequence chromatograms is indicated by a red arrow, and individuals carrying heterozygous (+/−), WT (+/+), or homozygous (−/−) *MYO15A* mutations are indicated. (b) Audiograms of the family carrying *MYO15A* mutation. Note that the members harboring a homozygous mutation all have bilateral profound non-syndromic sensorineural hearing loss, while those harboring heterozygous or WT mutation have normal hearing. The temporal bone HRCT for the proband shows that there is no inner ear malformations. (c) Scheme for the structure of human MYO15A and multiple sequence alignments of its homologs by genedoc32 software. The red arrow indicates the position of the novel mutation found in this study.

of *MYO15A*. The c. 2482C>T mutation was a highly suspected pathogenic mutation (PVS1 + PM2 + PP1 + PP3) according to ACMG guidelines; the mutation changed a highly conserved 828 arginine with a stop codon at the N-terminal extension domain of MYO15A, leading to a reduction of 2703 amino acids (aa) compared with the wild type (3530 aa). The Sanger sequence analysis of *MYO15A* was subsequently carried out among five affected patients and five unaffected members of this family. This potentially novel c. 2482C>T homozygous mutations were identified in five affected patients, while heterozygous mutations were identified in four of five unaffected subjects and only one unaffected member (II-7) with no *MYO15A* mutation (Figure 1a,b). There were no other sequence changes among these individuals. We further screened the *MYO15A* c.2482C>T mutation in 861 genetically unrelated deaf probands and 200 unaffected hearing-normal individuals using Sanger sequencing. We found that the c. 2482C>T mutation was absent in all these individuals. At the same time, the c. 2482C>T mutation frequency was 0 on the Genome AD website.

3.2 | Characterization of iPSCs

Primary fibroblasts were obtained from skin punch biopsies of the proband (II-2) and his sister (II-7). The methodology for the iPSC generation to operate was followed; approximately 15 days later, human iPSC-like colonies with a high nuclear-cytoplasmic ratio could be observed. Single colonies were then selected for further separate subculture (Figure 2a). We then conducted a series of experiments to verify the fully characterized generated putative iPSC lines (Figure 2). Alkaline phosphatase (AP) staining were positive in two putative iPSC lines. RT-PCR indicated that iPSC endogenous marker genes (*OCT4*, *SOX2*, *KLF4*, *NANOG*, and *c-MYC*) were expressed in the two putative iPSC lines, whereas most genes were silenced in fibroblast. Immunocytochemistry revealed that two putative iPSC lines expressed iPSC markers *OCT4*, *SOX2*, *NANOG*, *SSEA4*, and *TRA-1-60*. Embryoid bodies (EBs) were formed after an 8-day suspension culture of these putative iPSCs, and then an 8-day adherent culture later, specific marker genes such as *Brach*, *AFP*, and *PAX6* were detected. In addition, each teratoma derived from these putative iPSCs had a characteristic of the three germ layers in vivo (the gut epithelium for endoderm, cartilage for mesoderm, and retinal pigment for ectoderm). The mycoplasma testing results showed that there was no mycoplasma contamination in both iPSC cell lines. The STR testing results indicated that two iPSCs matched 100% with their corresponding fibroblast cell lines. These results showed that we had successfully generated two iPSC lines with full characterizations, and it is noteworthy that the *MYO15A* mutation did not affect the totipotency of iPSCs.

3.3 | Potentials of iPSCs to Differentiate Into Inner Ear Hair Cells

Subsequently, multiple experiments were performed to detect the potential of these iPSCs to differentiate into inner ear hair cells. The early otic markers including *PAX2*, *PAX8*, *SOX2*, and *Nestin* were detected in OEPs induced from the two iPSC lines (immunofluorescence staining results were not shown). They also expressed other early otic marker genes, including *GATA3*, *EYA1*, *SIX1*, and *DLX5* (Figure 3a). There was no significant difference in the otic gene expression between the two otic progenitors.

The hair cell marker genes, *ATOH1*, *BRN3C*, *MYO7A*, and *ESPN*, were all detected in the induced hair cell-like cells by gene expression analysis (Figure 3b).

3.4 | Morphology and Function of the Induced Hair Cell-Like Cells

The results of SEM showed that the induced cells also grew stereocilia-like structures based on microvilli. Notably, the stereocilia on the hair cell-like cells induced from II-2-iPSCs were significantly more sparse than those induced from II-7-iPSCs under SEM ($p < 0.0001$) (Figure 4).

To further figure out the effect of *MYO15A* mutation on hair cell-like cells, we performed RT-qPCR analysis for *MYO15A* using total RNA isolated from hair cell-like cells. The mRNA level of *MYO15A* was 6.9-fold lower in hair cell-like cells derived from II-2 than those from II-7 (Figure 5). This decrease may be caused by a nonsense-mediated decay due to the premature stop codon in exon 2 (Lejeune 2022).

4 | Discussion

MYO15A is essential for the mechanotransduction function of cochlear hair cells, and abnormally short stereocilia bundles and diminished staircase were observed in the MYO15A-deficient mouse (shaker-2) (Liang et al. 1999; Probst et al. 1998; Wakabayashi et al. 1998). The MYO15A is one of the unconventional myosins with 3530 amino acids, which contain seven kinds of domains, including a large N-terminal extension domain, a motor domain, two IQ motifs and a predicted third IQ, two MyTH4 domains, two FERM domains, an SH3 domain, and a PDZ ligand (Rehman et al. 2016). MYO15A can interact with the PDZ domain of Whirlin and Eps8, which are essential for normal hearing and transports them to the tip of stereocilia to form a complex; the complex can promote the crucial transformation of microvilli into mature stereocilia (Belyantseva et al. 2005). The motor domain composed of ATP- and actin-binding sites can produce force and move actin filaments (Anderson et al. 2000). Although the biological function of the N-terminal extension is unknown, Nal et al. (2007) reported that isoform 1of MYO15A with the N-terminal extension was necessary for normal auditory function. Therefore, it is not surprising that the MYO15A variant will lead to stereocilia dysfunction related to severe-to-profound deafness. In this study, we identified a novel *MYO15A* mutation c.2482C>T (p.Arg828*) in a Chinese Uygur family with NSHL; the potentially novel mutation was segregated with the disease. The p.Arg828* mutation is located in the N-terminal extension domain of MYO15A and affected the highly conserved 828 arginine. It also resulted in a 2703 amino acid reduction compared to wild type. The mutation only appeared in members with impaired hearing of this family in a homozygous form but absent in 200 subjects with normal hearing. The dysfunctions of inner hair cells were considered to be caused by the MYO15A deficiency and subsequently led to hearing loss.

Studies have shown that the hearing loss caused by the *MYO15A* gene mutation was complex. To date, more than 180 variants of *MYO15A* associated with hearing loss phenotypes have been reported, and most of *MYO15A* variants were located in the motor domain (Zhang et al. 2019). Initially, most *MYO15A* variants located in the non-N-terminal extension domain were reported to be related to the bilateral congenital severe-to-profound sensorineural deafness at all frequencies (Liburd et al. 2001), while variants in the N-terminal extension domain only cause a light hearing loss with residual hearing at low frequencies (Nal et al. 2007). With the further research on the *MYO15A* gene, some variants that affect the functional domains were observed to be associated with a milder hearing loss, and variants located in the N-terminal domain cause a severe-to-profound auditory phenotype rather than a milder phenotype; a delayed or progressive moderate-to-severe auditory phenotype has also been reported (Cengiz et al. 2010; Chang et al. 2018; Li et al. 2016). In this paper, we reported one homozygous mutation in exon 2

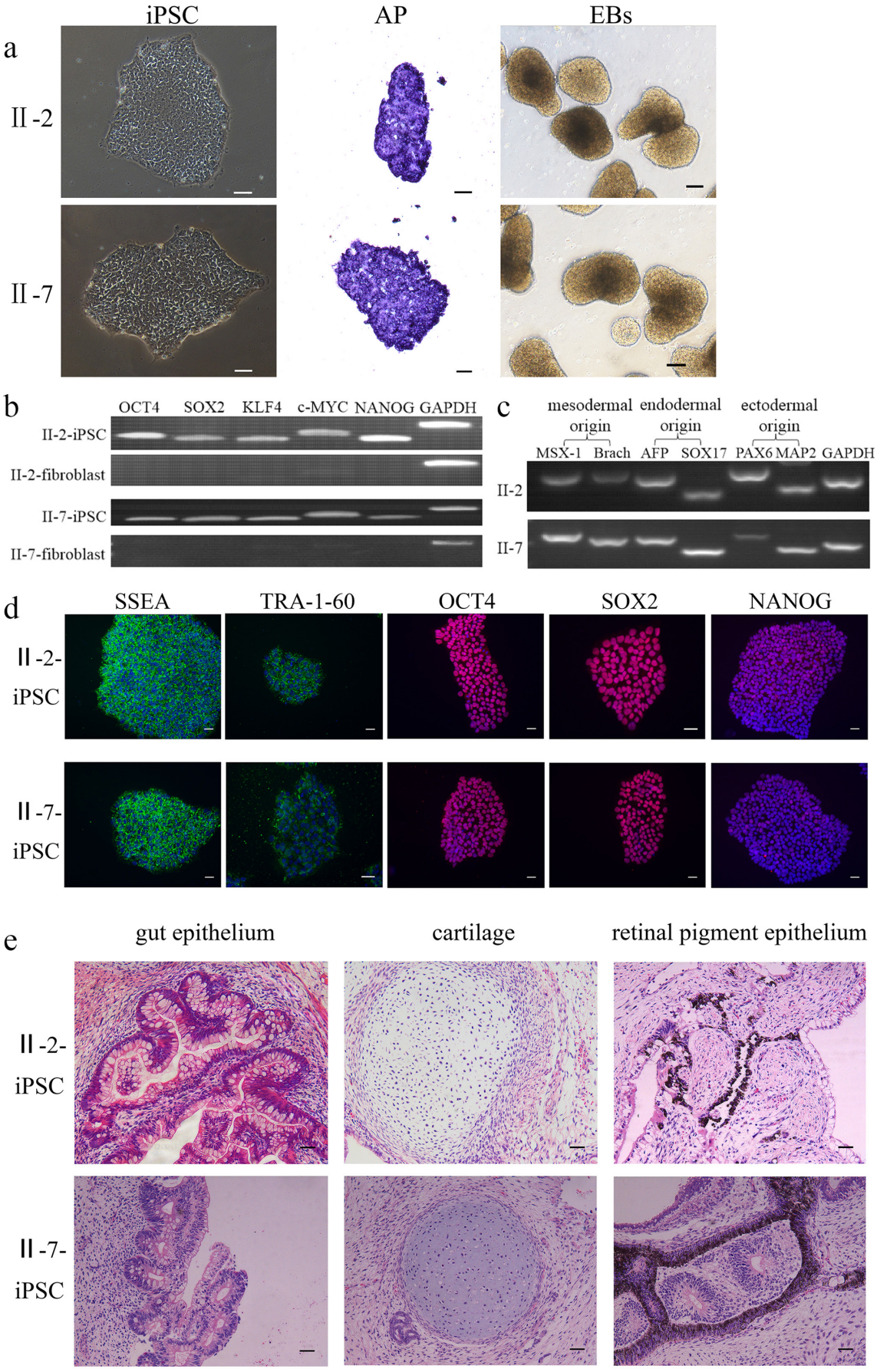

FIGURE 2 | Legend on next page.

FIGURE 2 | Characterization of iPSCs from proband (II-2) and his sister (II-7) without the *MYO15A* mutation. (a) Phase contrast microscopy of derived iPSCs, AP staining of the two putative iPSCs, and embryoid bodies formed after 8 days of suspension culture. Scale bars: 400 μm in EB images; 200 μm in the other images. (b) The identification of the two iPSC line endogenous marker genes (*OCT4*, *SOX2*, *KLF4*, *NANOG*, and *c-MYC*) by RT-PCR. Expression of all endogenous marker genes was detected in the two iPSCs, whereas most genes were silenced in fibroblast. (c) RT-PCR analysis of the expression of marker genes for the three germ layers of embryoid bodies after a subsequent 8-day adherent culture. *AFP* and *SOX17* for the endoderm, *Brachyury* and *MSX-1* for the mesoderm, and *PAX6* and *MAP2* for the ectoderm. (d) Immunostaining for pluripotent markers *SSEA4*, *TRA-1–60*, *OCT4*, *SOX2*, and *NANOG* in the two putative iPSCs. Nuclei were stained with DAPI (blue). Scale bars: 100 μm. (e) Teratomas formed from the NOD-SCID mice and stained with hematoxylin and eosin. The gut epithelium for endoderm, cartilage for mesoderm, and retinal pigment for ectoderm were observed. Scale bars: 200 μm.

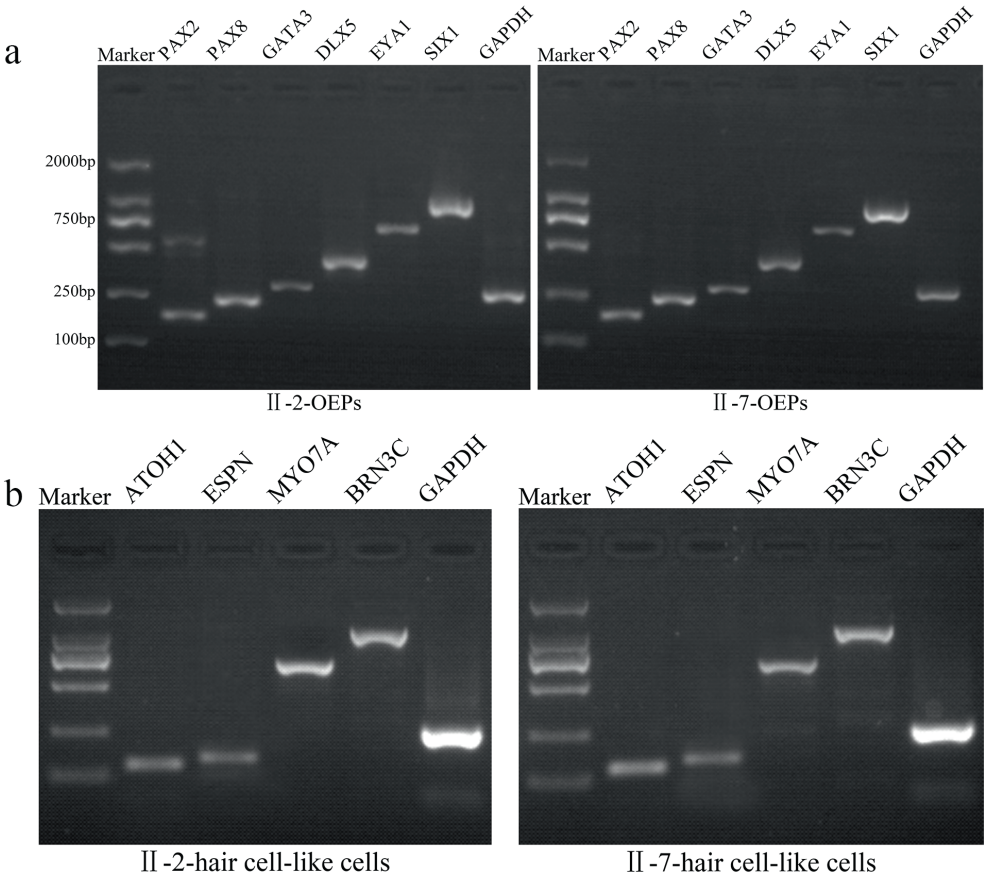

FIGURE 3 | Potentials of iPSCs to differentiate into inner ear hair cells. (a) RT-PCR analysis of the expression of early otic progenitor marker genes. *PAX2*, *PAX8*, *GATA3*, *DLX5*, *EYA1*, and *SIX1* were detected in the two iPSCs induced toward the otic epithelial progenitors (OEPs). (b) The gene expression analysis of hair cell marker genes, including *ATOH1*, *ESPN*, *MYO7A*, and *BRN3C*. These two induced hair cell-like cells expressed the above marker genes.

encoding the N-terminal domain, which showed congenital profound sensorineural deafness at all frequencies; this has rarely been reported in the previous literature. It is reported that two alternatively spliced transcripts exist in MYO15A; isoform 2 lacks exon 2, while isoform 1 contains a large N-terminal extension (Liang et al. 1999). Fang et al. (2015) revealed that isoform 2 was predominantly expressed during the early development of the newborn, but isoform 1 gradually tended to express in postnatal cochlear, which was required for the postnatal maintenance of shorter row mechanotransducing stereocilia. Recent study also demonstrated that the 133-kDa N-terminal domain was indispensable for normal hearing in humans (Nal et al. 2007). In our study, the c.2482C>T homozygous mutation identified at the N-terminal domain leads to the deletion of intact isoform 1 of MYO15A, and the five patients with mutant alleles in JX81 were all congenital profound preverbal deafness, indicating that isoform 1 seriously affects the physiological function of hair cell stereocilia and finally leads to deafness.

The inner ear hair cells function as mechanosensors to convert sound waves into electrochemical activities of neural cells (Roy and Perrin 2018). However, hair cells in mammals are non-regenerative. Changes in the number and structure of hair cell stereocilia can result in the decline or even loss of auditory function. The establishment of the iPS cell technology has broken the dependence on embryo-derived stem cells in the field of stem cell research and provided an important theoretical support and technical guarantee for the induction and regenerative medicine research of patient-specific stem cells. In this study, fibroblasts from a patient with *MYO15A* c. 2482C>T homozygous mutation

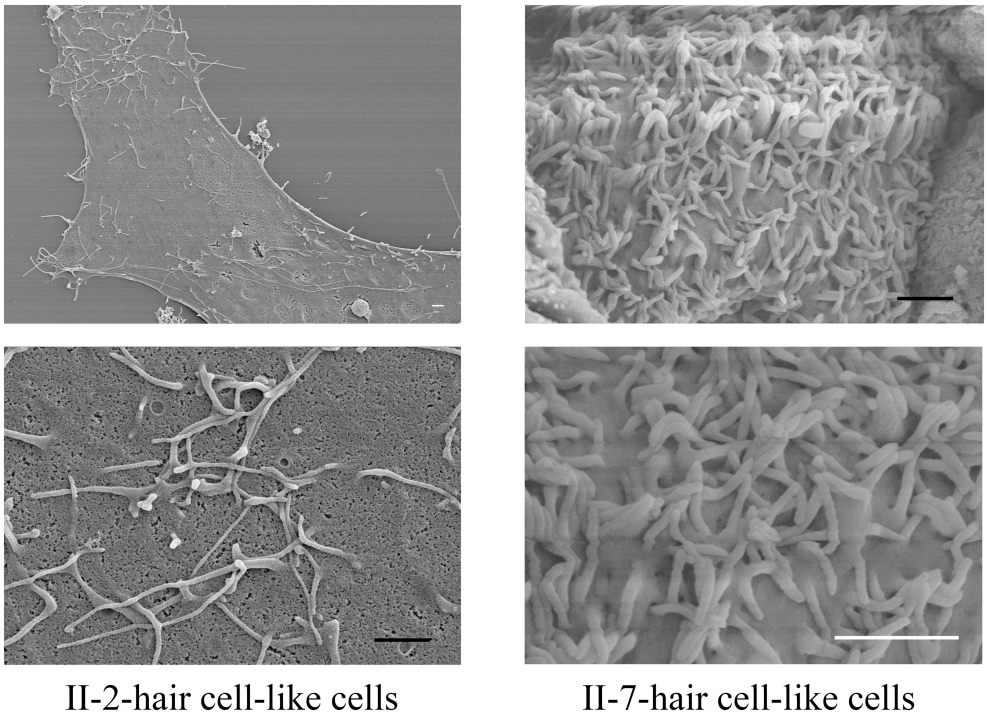

FIGURE 4 | SEM of hair cell-like cells derived from iPSCs. Multiple areas of hair cell-like cells (per $1\,\mu m^2$) were counted using ImageJ software, ($n = 5$). Data are mean ± SEM of quintuplicate. The result showed a significant statistical difference ($p < 0.0001$) by an unpaired Student's t test. Scale bars: $1\,\mu m$.

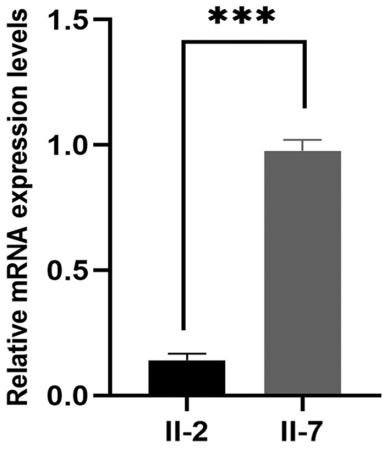

FIGURE 5 | The relative mRNA expression levels of *MYO15A* were analyzed in differentiated hair cell-like cells. The housekeeping gene, *GAPDH*, was used as an internal reference. *** represents a high statistically significant difference ($p < 0.001$) by an unpaired Student's *t* test.

were successfully induced into iPSCs; then, these were induced to differentiate toward inner ear hair cells to study the pathogenesis of *MYO15A* mutation. Our results revealed that the *MYO15A* mutation did not affect the totipotency of iPSCs.

Using iPSCs, we successfully demonstrated that homozygous *MYO15A* (c.2482C>T) alleles can hinder stereocilium differentiation. The II-2-iPSCs develop stereocilia much sparsely compared with the II-7-iPSCs (Figure 4). However, a mouse model lacking MYO15A isoform 1 showed morphologically normal stereocilia with profound hearing loss (Fang et al. 2015), which was different from our results for an unknown reason. Presently, it is still challenging to use iPSCs to predict the consequence of genetic variation because induced stereocilia do not reproduce the morphology and functions of in vivo stereocilia. We speculate that iPSCs may be a useful model for genetic diagnosis in the future if technical advances allow us to induce more physiological stereocilia.

In conclusion, the novel homozygous c.2482C>T of *MYO15A* reduced the MYO15A protein by 2703 amino acids compared with wild type, affected the integrity of isoform 1 of MYO15A, and ultimately led to deafness. These findings not only expand the spectrum of *MYO15A* pathogenic variants but also prompt further research on the mechanisms of deafness caused by MYO15A, especially on the effects of isoform 1 on hair cell growth and development.

Author Contributions

All authors contributed to the study conception and design. Material preparation, data collection, and analysis were performed by Yanli Wang, Zhipeng Nie, Yong Li, Xingjian Chen, Huan Tan, and Jiong Dang. The first draft of the manuscript was written by Yanli Wang and Zengping Liu. The review and editing of the manuscript were performed by Baicheng Xu, Yiming Zhu, and Shihong Duan. The final approval of the manuscript was performed by Yufen Guo and Minxin Guan, and all authors commented on previous versions of the manuscript. All authors read and approved the final manuscript.

Acknowledgments

We are indebted to the participating deafness patients and their parents for their cooperation.

Ethics Statement

This study was approved by the ethics committee of Lanzhou University Second Hospital (No. 2023A-233).

Consent

This study was conducted with the informed consent of participating deafness patients and their parents.

Conflicts of Interest

The authors declare no conflicts of interest.

Data Availability Statement

The data and materials used to support the findings of this study are available from the corresponding author upon request.

References

Anderson, D. W., F. J. Probst, I. A. Belyantseva, et al. 2000. "The Motor and Tail Regions of Myosin XV Are Critical for Normal Structure and Function of Auditory and Vestibular Hair Cells." *Human Molecular Genetics* 9, no. 12: 1729–1738.

Belyantseva, I. A., E. T. Boger, S. Naz, et al. 2005. "Myosin-XVa Is Required for Tip Localization of Whirlin and Differential Elongation of Hair-Cell Stereocilia." *Nature Cell Biology* 7, no. 2: 148–156.

Bitner-Glindzicz, M. 2002. "Hereditary Deafness and Phenotyping in Humans." *British Medical Bulletin* 63: 73–94.

Cengiz, F. B., D. Duman, A. Sirmaci, et al. 2010. "Recurrent and Private MYO15A Mutations Are Associated With Deafness in the Turkish Population." *Genetic Testing and Molecular Biomarkers* 14, no. 4: 543–550.

Chang, M. Y., C. Lee, J. H. Han, et al. 2018. "Expansion of Phenotypic Spectrum of MYO15A Pathogenic Variants to Include Postlingual Onset of Progressive Partial Deafness." *BMC Medical Genetics* 19, no. 1: 29.

Chen, J. R., Z. H. Tang, J. Zheng, et al. 2016. "Effects of Genetic Correction on the Differentiation of Hair Cell-Like Cells From iPSCs With MYO15A Mutation." *Cell Death and Differentiation* 23, no. 8: 1347–1357.

Chen, W., N. Jongkamonwiwat, L. Abbas, et al. 2012. "Restoration of Auditory Evoked Responses by Human ES-Cell-Derived Otic Progenitors." *Nature* 490, no. 7419: 278–282.

Cui, L., J. Zheng, Q. Zhao, et al. 2020. "Mutations of MAP1B Encoding a Microtubule-Associated Phosphoprotein Cause Sensorineural Hearing Loss." *JCI Insight* 5, no. 23: e136046.

Fang, Q., A. A. Indzhykulian, M. Mustapha, et al. 2015. "The 133-kDa N-Terminal Domain Enables Myosin 15 to Maintain Mechanotransducing Stereocilia and Is Essential for Hearing." *eLife* 4: 4.

Farjami, M., R. Assadi, F. Afzal Javan, et al. 2020. "The Worldwide Frequency of MYO15A Gene Mutations in Patients With Non-Syndromic Hearing Loss: A Meta-Analysis." *Iranian Journal of Basic Medical Sciences* 23, no. 7: 841–848.

Hudspeth, A. J. 2014. "Integrating the Active Process of Hair Cells With Cochlear Function." *Nature Reviews Neuroscience* 15, no. 9: 600–614.

Lejeune, F. 2022. "Nonsense-Mediated mRNA Decay, a Finely Regulated Mechanism." *Biomedicine* 10, no. 1: 141.

Li, W., L. Guo, Y. Li, et al. 2016. "A Novel Recessive Truncating Mutation in MYO15A Causing Prelingual Sensorineural Hearing Loss." *International Journal of Pediatric Otorhinolaryngology* 81: 92–95.

Liang, Y., A. Wang, I. A. Belyantseva, et al. 1999. "Characterization of the Human and Mouse Unconventional Myosin XV Genes Responsible for Hereditary Deafness DFNB3 and Shaker 2." *Genomics* 61, no. 3: 243–258.

Liburd, N., M. Ghosh, S. Riazuddin, et al. 2001. "Novel Mutations of MYO15A Associated With Profound Deafness in Consanguineous Families and Moderately Severe Hearing Loss in a Patient With Smith-Magenis Syndrome." *Human Genetics* 109, no. 5: 535–541.

Lowry, W. E., L. Richter, R. Yachechko, et al. 2008. "Generation of Human Induced Pluripotent Stem Cells From Dermal Fibroblasts." *Proceedings of the National Academy of Sciences of the United States of America* 105, no. 8: 2883–2888.

Nal, N., Z. M. Ahmed, E. Erkal, et al. 2007. "Mutational Spectrum of MYO15A: The Large N-Terminal Extension of Myosin XVA Is Required for Hearing." *Human Mutation* 28, no. 10: 1014–1019.

Okita, K., Y. Matsumura, Y. Sato, et al. 2011. "A More Efficient Method to Generate Integration-Free Human iPS Cells." *Nature Methods* 8, no. 5: 409–412.

Oshima, K., K. Shin, M. Diensthuber, A. W. Peng, A. J. Ricci, and S. Heller. 2010. "Mechanosensitive Hair Cell-Like Cells From Embryonic and Induced Pluripotent Stem Cells." *Cell* 141, no. 4: 704–716.

Park, I. H., P. H. Lerou, R. Zhao, H. Huo, and G. Q. Daley. 2008. "Generation of Human-Induced Pluripotent Stem Cells." *Nature Protocols* 3, no. 7: 1180–1186.

Probst, F. J., R. A. Fridell, Y. Raphael, et al. 1998. "Correction of Deafness in Shaker-2 Mice by an Unconventional Myosin in a BAC Transgene." *Science* 280, no. 5368: 1444–1447.

Redowicz, M. J. 1999. "Myosins and Deafness." *Journal of Muscle Research and Cell Motility* 20, no. 3: 241–248.

Rehman, A. U., J. E. Bird, R. Faridi, et al. 2016. "Mutational Spectrum of MYO15A and the Molecular Mechanisms of DFNB3 Human Deafness." *Human Mutation* 37, no. 10: 991–1003.

Roy, P., and B. J. Perrin. 2018. "The Stable Actin Core of Mechanosensory Stereocilia Features Continuous Turnover of Actin Cross-Linkers." *Molecular Biology of the Cell* 29, no. 15: 1856–1865.

Scheffer, D. I., D. S. Zhang, J. Shen, et al. 2015. "XIRP2, An Actin-Binding Protein Essential for Inner Ear Hair-Cell Stereocilia." *Cell Reports* 10, no. 11: 1811–1818.

Sennaroglu, L., and M. D. Bajin. 2017. "Classification and Current Management of Inner ear Malformations." *Balkan Medical Journal* 34, no. 5: 397–411.

Takahashi, K., and S. Yamanaka. 2006. "Induction of Pluripotent Stem Cells From Mouse Embryonic and Adult Fibroblast Cultures by Defined Factors." *Cell* 126, no. 4: 663–676.

Wakabayashi, Y., Y. Takahashi, Y. Kikkawa, et al. 1998. "A Novel Type of Myosin Encoded by the Mouse Deafness Gene Shaker-2." *Biochemical and Biophysical Research Communications* 248, no. 3: 655–659.

Wang, A., Y. Liang, R. A. Fridell, et al. 1998. "Association of Unconventional Myosin MYO15 Mutations With Human Nonsyndromic Deafness DFNB3." *Science* 280, no. 5368: 1447–1451.

Wen, J., C. He, Y. Feng, et al. 2021. "Establishment of an iPSC Line (CSUXHi004-A) From a Patient With Waardenburg Syndrome Type I Caused by a PAX3 Splice Mutation." *Stem Cell Research* 53: 102300.

Zhang, J., J. Guan, H. Wang, et al. 2019. "Genotype-Phenotype Correlation Analysis of MYO15A Variants in Autosomal Recessive Non-Syndromic Hearing Loss." *BMC Medical Genetics* 20, no. 1: 60.